HAL open science

Synthesis and evaluation of a novel class of ethacrynic acid derivatives containing triazoles as potent anticancer agents

Abdelmoula El Abbouchi, Nabil El Brahmi, Marie-Aude Hiebel, Jérôme Bignon, Gérald Guillaumet, Franck Suzenet, Saïd El Kazzouli

To cite this version:

Abdelmoula El Abbouchi, Nabil El Brahmi, Marie-Aude Hiebel, Jérôme Bignon, Gérald Guillaumet, et al.. Synthesis and evaluation of a novel class of ethacrynic acid derivatives containing triazoles as potent anticancer agents. Bioorganic Chemistry, 2021, 115 (2), pp.105293. 10.1016/j.bioorg.2021.105293 . hal-03421113

HAL Id: hal-03421113

https://hal.science/hal-03421113v1

Submitted on 16 Oct 2023

HAL is a multi-disciplinary open access archive for the deposit and dissemination of scientific research documents, whether they are published or not. The documents may come from teaching and research institutions in France or abroad, or from public or private research centers.

L'archive ouverte pluridisciplinaire **HAL**, est destinée au dépôt et à la diffusion de documents scientifiques de niveau recherche, publiés ou non, émanant des établissements d'enseignement et de recherche français ou étrangers, des laboratoires publics ou privés.

Distributed under a Creative Commons Attribution - NonCommercial 4.0 International License

Version of Record: https://www.sciencedirect.com/science/article/pii/S0045206821006702
Manuscript_393a97ccf5f5c7134e959e5df1f4580f

Synthesis and evaluation of a novel class of ethacrynic acid derivatives containing triazoles as potent anticancer agents

Abdelmoula El Abbouchi [a,b], Nabil El Brahmi [a], Marie-Aude Hiebel [b], Jérôme Bignon [c], Gérald Guillaumet [a,b*], Franck Suzenet [b*], Saïd El Kazzouli [a*]

[a] Euromed Research Center, Engineering School of Biomedical and Biotechnology, Euromed University of Fes (UEMF)–Route de Meknès, 30000 Fez, Morocco.
[b] Institut de Chimie Organique et Analytique, Université d'Orléans, UMR CNRS 7311, BP 6759, Orléans cedex 2 54067, France
[c] Institut de Chimie des Substances Naturelles, CNRS, Université Paris-Saclay, Gif-sur-Yvette,France

Abstract:

For unmet clinical needs, a novel class of ethacrynic acid (**EA**) derivatives containing triazole moieties (**3a-i** and **8**) were designed, synthesized and evaluated as new anticancer agents. The *in vitro* anti-proliferative activities were assessed first on HL60 cell line and in a second stage, the two selected compounds **3a** and **3c** were tested on a panel of human cancer cell lines (A549, MCF7, PC3, U87-MG, SKOV3 and HCT116) and on a normal cell line (MCR5). Compound **3c** exhibited very good antitumor activities with IC_{50} values of 20.2, 56.5 and 76.8 nM against A549, PC3 and U87-MG cell lines respectively, which is 2.8- and 1.3-fold more active than doxorubicin on A549 and U87-MG cancer cells, respectively. In addition, compound **3c** displays a very good safety index (SI) of 82 fold for A549. Compound **3a** showed also good IC_{50} values of 50 nM on both A549 and PC3 cells and lower selectivity compared to **3c** for A549 and PC3 *vs.* MCR5 with SI of 33 and 18 fold, respectively. The measurement of mitochondrial membrane potential on HCT116 cells after treatments by either **3a** or **3c** showed that both compounds induced mitochondrial dysfunctions causing thus caspase-induced apoptosis.

Keywords: Ethacrynic acid, cytotoxic activity, triazole, anticancer agents.

1. Introduction:

Cancer is the second leading cause of death with approximately 10 million deaths in 2020 [1]. The most common cancers based on the number of the cancer cases are: lung, breast, colorectal, prostate, skin and stomach cancer [2]. Different treatments are available depending on cancer type and its progress state. For instance, radiation, targeted or

© 2021 published by Elsevier. This manuscript is made available under the CC BY NC user license
https://creativecommons.org/licenses/by-nc/4.0/

hormone therapy, immunotherapy, and chemotherapy are commonly used [3]. In some cases, only one approach is needed to achieve recovery. Unfortunately, in most of the cases, a combination of two or more treatments is required and involved most of the time chemotherapy. However, chemotherapy not only suffers from sides effects such as the fatigue, hair loss, anemia eg…, it mainly encounters tumor resistance [4]. Thus, the development of new treatments especially for resistant tumors against chemotherapeutic agents is imperatively needed [4].

It is well established that microsomal glutathione S-transferase 1 (mGST1) and glutathione S-transferase p (GST p) which are overexpressed in cancer cells confer resistance against a number of cytostatic drugs [5–10]. To tackle this problem, the development of treatments based on ethacrynic acid (**EA**), Edecrin®, known as inhibitor of GST p through nucleophilic addition of thiols on the α,β-unsaturated carbonyl unit of **EA**, appears to be very promising [11,12]. It is important to note that its combination with several known anticancer agents such as cisplatin®, [13,14] chlorambucil®, melphalan®, mitomycin C®, and doxorubicin®, was studied showing enhanced *in vitro* cytotoxic activities [15]. In addition, an upgrading in cytotoxic activity *in vivo* was observed when **EA** was used as an adjuvant in clinical trials against multiple myeloma [12,16–18]. Moreover, the **EA** association with lenalidomide® and thalidomide® revealed an improved *in vivo* anti-proliferative activity [16,19]. Importantly, **EA** in combination with thiotepa® was under a phase I clinical trial for the treatment of malignant solid tumors [20].

In the meantime, several analogs of **EA** were synthesized in order to improve the anti-proliferative activity and / or the capacity to inhibit the GST p. So far, the structure-activity relationship studies clearly showed that all the modifications or reduction of the unsaturated double bond and / or the carbonyl unit abolished the anti-proliferative activity [21]. However, carboxylic group modifications by formation of simple amides or their analogs [21,22–24], oxadiazole [25,26], thiazole analogs [27], esters [11,28,29], as well as sulfonamides [30], showed a significant improvement of the anti-proliferative activities with IC_{50} ranging between 25 nM and 20 µM *vs.* ~50 µM for **EA**.

Previous efforts from our group underlined that the substitution of the carboxylic group by either 2-(4-substituted (phenyl)ethanamine or 4-(4-substituted phenyl)piperazine moieties generated compounds that exhibited moderate to strong anti-proliferative activities against human cancer cell lines namely, tumor KB (epidermal carcinoma) and leukemia HL60 (promyelocytic) cells [21]. Moreover, some further insights into the mode of action of the **EA** analogs suggested a more complex behavior than the sole inhibition of GST p. The reported **EA** derivatives induced primarily apoptosis without activation of necrosis through a caspase activation, a phenomenon that might help to avoid tumor resistances [21]. Very recently, we demonstrated that the substitution of the carboxylic acid by sulfonamides linked *via* three

different types of linkers (specifically 2-ethylenediamine, piperazine and 4-aminopiperidine were synthesized) led to **EA** derivatives with good anti-proliferative activities against a panel of cancer cell lines with IC_{50} values in a nanomolar range [30].

With the aim of finding more active and selective **EA** derivatives and by taking advantage of the bioisosterism between the amide et triazole moieties, we report in this current study the synthesis of a novel class of **EA** analogs bearing triazole moieties readily obtained by using Huisgen 1,3-dipolar cycloaddition. The synthetized compounds are biologically evaluated *in vitro* for their anti-proliferative activity against different cancer and normal cells. In addition, *via* the measurement of mitochondrial membrane potential, the mechanism of action involving caspase activation was established on HCT116 cells through mitochondrial dysfunction. Finally, the determination of intracellular GSH level, an important marker of cell viability, was also realized on HCT116 cells.

2. Results and discussion

2.1. Chemistry

The synthetic route of new **EA** derivatives containing triazoles **3a-i** is outlined in Scheme 1. First, commercially available **EA** was condensed with propargylamine in the presence of 1-ethyl-3-(3-dimethylaminopropyl)carbodiimide (EDC), 4-(dimethylamino)pyridine (DMAP) and 1-hydroxybenzotriazole (HOB*t*) in dry DMF under argon atmosphere to provide **1**. The intermediates **2** were smoothly obtained using methods previously reported in the literature [31,32]. Then, a copper (I)-catalyzed Azide-Alkyne Cycloaddition (CuAAC) reaction was performed between compound **1** and intermediate **2** in the presence of $CuSO_4.5H_2O$ and sodium ascorbate in *t*-butyl alcohol and water (2/1) at 60°C. The reaction enabled to achieve **EA**-triazole derivatives **3a-i** in moderate to good yields (36-79%) (Scheme 1). All the synthesized compounds were fully characterized by ^{1}H NMR, ^{13}C NMR, HRMS, IR and melting point.

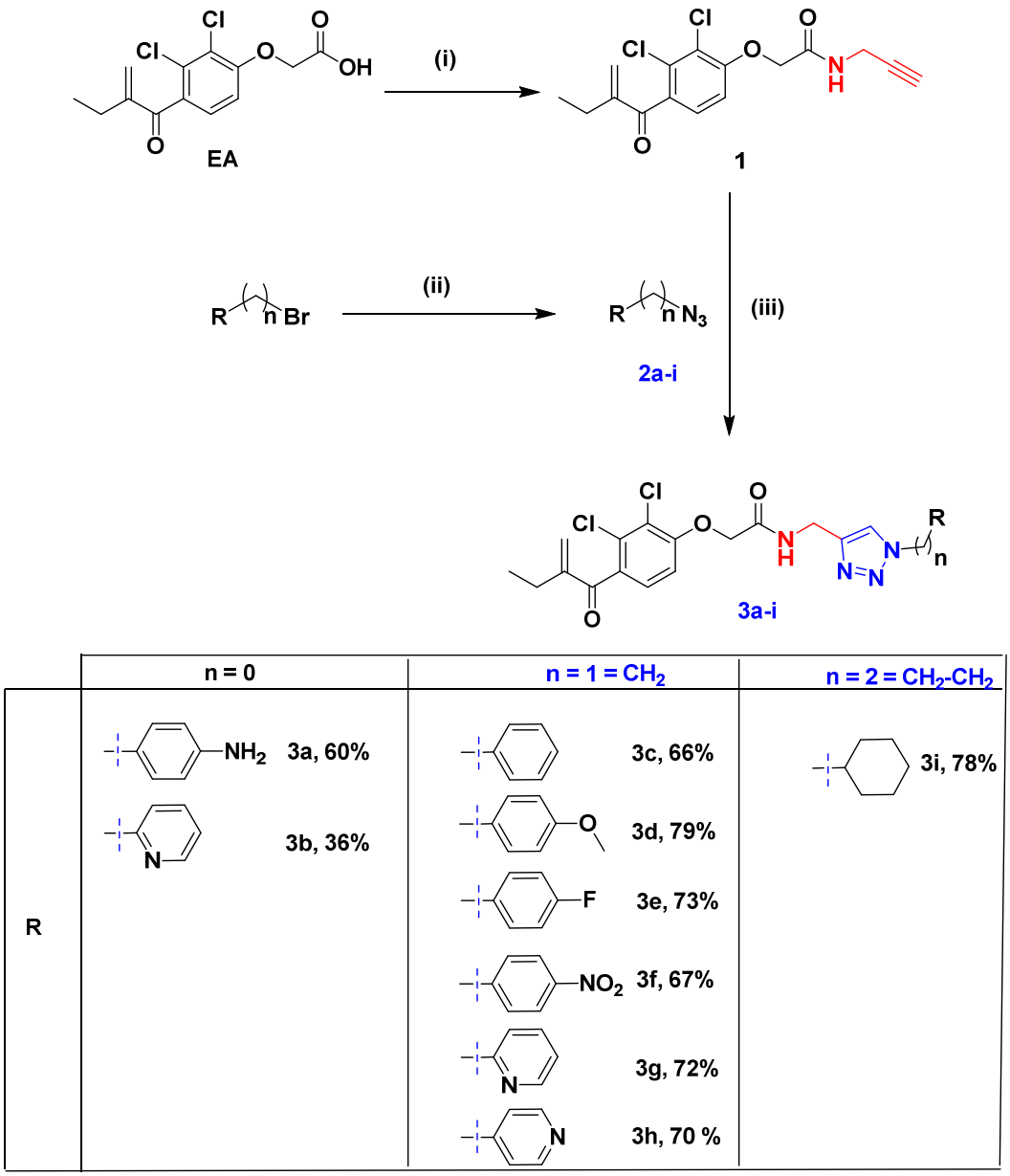

Scheme 1. Synthesis of **EA** derivatives **3a-i.** Reagents and conditions: (i) Propargylamine, DMAP, DMF, N_2 or argon, 0°C, 16 h ; (ii) Case n=1,2,3 : NaN_3, acetone/H_2O, rt, 8 h ; Case n=0 : sodium ascorbate, CuI, DMEDA, NaN_3, Ethanol/H_2O, reflux, 12 h ; (iii) Sodium ascorbate, $CuSO_4$, $5H_2O$, *t*BuO*H*/H_2O (2/1), 60°C, 12 h.

Additionally, since the triazole group is known to be a bioisoster of the amide group, [33] we found interesting to study this bioisostery effect on this **AE** series and therefore compound **8** was synthesized using a four-step synthetic route detailled in Scheme 2. Dichloromethoxybenzene (**4**) was acylated with of butanoyl chloride by a Friedel-Crafts acylation in the presence of of aluminium chloride powder ($AlCl_3$) in anhydrous DCM at 0°C for 2 h. Then, the intermediate was treated without purification by an additional amount of of

$AlCl_3$ in refluxing DCM for 5 h to afford the intermediate **5** in 78% yield [34]. Subsequently, the phenol (**5**) was alkylated by of propargyl bromide in THF for 24 h in the presence of potassium *tert*-butoxide and a catalytic amount of potassium iodide to afford compound **6** in a good yield (85%). In the third step, an aldol condensation reaction in the presence of formaldehyde and potassium carbonate was applied in a mixture of ethanol/water (1/1) for 24 h to give compound **7** in 33% yield. In the final step, compound **8** was obtained by a CuAAC reaction in 62% yield according to procedure used to prepare compound **3** (Scheme 2). All the synthesized compounds and intermediates were fully characterized by ^{1}H NMR, ^{13}C NMR, HRMS, IR and melting point.

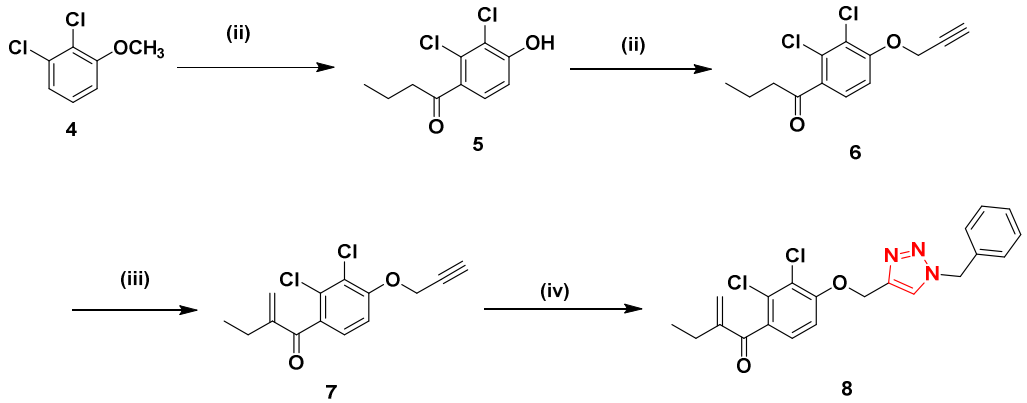

Scheme 2. Synthesis of compound **8**. Reagents and conditions : (i) First : butyl chloride, $AlCl_3$, DCM, 0°C, 2 h ; Then : $AlCl_3$, DMF, reflux, 5 h ; (ii) Propargyl bromide, *t*BuOK, KI, THF, 60°C, 24 h ; (iii) 37% CH_2O in H_2O, K_2CO_3, EtOH/H_2O (1/1), reflux, 24 h ; (iv) **2C**, Sodium scorbate, $CuSO_4$. $5H_2O$, *t*BuOH/H_2O (2/1), 60°C, 12 h.

2.2. Biological study

All the newly synthesized **EA**-triazole derivatives and some intermediates were evaluated for their *in vitro* inhibitory activity toward HL60 cells using MMT test. **EA** was used as a positive control, with the results expressed as half-maximal inhibitory concentration (IC_{50}) values are presented in Table 1. The IC_{50} values are the average of at least three independent experiments.

Table 1. Anti-proliferative activities of **EA** and their derivatives**.**

Chemical structures	Compounds	n	R-	IC_{50} (HL60) µM
	3a	0	4-aminophenyl	0.31 ± 0.02
	3b	0	2-pyridyl-	1.73 ± 0.61

	3c	1	phenyl-	0.29 ± 0.05
	3d	1	4-methoxyphenyl	0.38 ± 0.04
	3e	1	4-flurophenyl	0.32 ± 0.04
	3f	1	4-nitrophenyl	0.66 ± 0.02
	3g	1	2-pyridiyl-	0.59 ± 0.02
	3h	1	4-pyridyl-	0.88 ± 0.09
	3i	2	cyclohexyl-	0.87 ± 0.08
	1			1.06 ± 0.008
	8			0.63 ± 0.09
	7			0.58 ± 0.04

As illustrated in Table 1 the tested compounds showed moderate to excellent anti-proliferative activity with IC_{50} values ranging from 0.29 to 1.73 µM, which indicated that introduction of triazole moieties to the **EA** framework efficiently enhanced the antitumor activities. We noticed that **3a**, **3c**, **3d** and **3e** were the most active compounds displaying very similar IC_{50} values on HL60. At this level, we decided to select only two compounds **3a** and **3c** for further investigations of their antiproleferative activities on various cancer and normal cell lines as well as of their mechanism of action. For this reason, we selected one compound in which the aryl group (R) is directly linked to triazole moiety (n = 0), and the best analog is compound **3a**. For the second compound we selected one compound having a methylene spacer (-CH_2-) between the aryl group and the triazole (n = 1). In this case, we selected the most efficient and less expensive, easier and cheaper compound in terms of its preparation (compound **3c**).

Thus, derivatives **3a** and **3c** exhibited promising activities against HL60 with IC_{50} values of 0.31 µM and 0.29 µM respectively (Figure 1). It is worth noting that compound **8** was slightly less cytotoxic than **3c** with IC_{50} of 0.63 µM *vs.* 0.29 µM for **3c**, indicating the positive effect of both amide and triazole linkers on the anti-proliferative activity.

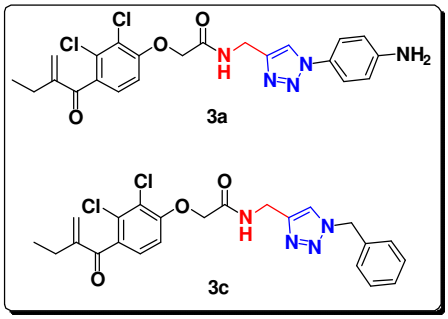

Figure 1. The chemical structures of **3a** and **3c.**

Next, we investigated the *in vitro* cytotoxicity of the two selected compounds **3a** and **3c** on a panel of cancer and normal cell lines representative of diverse tissues/organ tumors: human adenocarcinomic epithelial cell line (A549), human breast cancer cell line (MCF7), human prostate cancer cell line (PC3), human glioblastoma (U87-MG), ovarian carcinoma cells (SKOV3), human colon cancer cell line (HCT116). Moreover, to evaluate the safety index of our compounds, their effect on the proliferation of human lung fibroblasts (MCR5) as non-cancer cell line was also studied. The cytotoxicities in terms of IC_{50} obtained after 72 h of exposure are summarized in Table 2.

Table 2. Anti-proliferative activity of **EA** derivatives and doxorubicin (Doxo) upon various cancer human cells and normal cells.

	IC_{50} in nM						
Cells / Compds	**A549**	**MCF7**	**PC3**	**U87-MG**	**SKOV3**	**HCT116**	**MRC5**
3a	50.1 ± 8.7	107 ± 17.6	92.5 ± 10.7	460 ± 8.2	510 ± 20.4	700 ±90	1670 ± 170
3c	20.2 ± 1.9	132 ± 14.1	56.5 ± 5.8	76.8 ± 4.2	107±4.1	650 ± 150	1670 ± 210
Doxo	56.6 ± 0.84	120 ± 90	2.1 ± 0.03	99.6 ± 2.34	nc	90 ± 3	39.88 ± 1.22

nc: not calculated

The results enlisted in Table 2 showed that the selected compounds **3a** and **3c** displayed promising anti-proliferative activities. In comparison with doxorubicin (Doxo), **3c** appeared even more active on A549 and U87-MG cell lines while **3a** exhibited the same range of cytotoxicity on A549 and MCF7 cell lines. Moreover, unlike Doxo, **3a** and **3c** were both active on SKOV3 cell line. While Doxo remained more active on PC3 cell line, **3a** and **3c** showed interesting IC_{50} values in nanomolar range (92.5 nM and 56.5 nM respectively). For HCT116 cancer cell line, compounds **3a** and **3c** were significantly less active than Doxo (IC_{50} = 90

nM) with IC_{50} values of 700 and 650 nM, respectively. However, above all, it is worth noting that **3a** and **3c** were remarkably less toxic on non-cancerous cells with IC_{50} around 1670 nM. By comparing the SAR of the **EA**-derivatives reported herein with our best analogs published to date (Figure 2) [21, 30], we can conclude that the replacement of the amide moiety by the triazole group led to a new and more promising **EA**-family in terms of the antiproleferative activity aspect, considering the increased selectivity for one or more cancer cell lines compared to **EA**-derivatives containing sulfonamides or amide groups. As previously noticed in the precedent studies, the nature of the aryl group used for the functionalization has slight impact on the antiproleferative activity as well as on cancer cell selectivity. For example, the compound **3c** showed an IC_{50} three fold lower against **A549** than compound **V** while compound **V** was more active on PC3 (IC_{50} = 24.8 nM) than **3c** (IC_{50} = 56.5 nM).

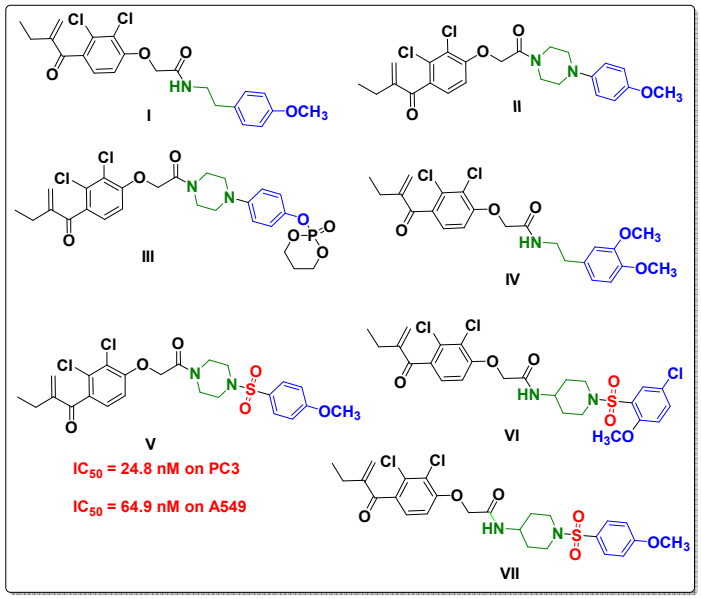

Figure 2. Chemical structures of previously reported **EA** analogues [21, 30]

The safety index of **3a** and **3c** was calculated for each cancerous cell line (SI, defined as the ratio of the IC_{50s} of noncancerous cells / IC_{50s} of cancer cells) and reported in Table 3. The results corroborated the well-known poor selectivity of doxorubicin and emphasized the selectivity of our compounds especially **3c** that exhibited good SI on A549 and moderate SI on PC3 and U87-MG cell lines.

Table 3. Safety index of **3a** and **3c.**

SI = MCR5/cancer / Compds	SI HL60	SI A549	SI MCF7	SI PC3	SI U87	SI SKOV3	SI HCT116
3a	5.38	**33.33**	**15.60**	**18.05**	3.63	3.27	2.38
3c	5.75	**82.67**	**12.65**	**29.55**	**21.74**	**15.60**	2.56
Doxo	3.98	0.70	0.33	19.08	0.40	NC	0.44

NC : not calculated

Meanwhile, the lipophilicity was calculated using Marvin application (ChemAxon). Compounds **3a** and **3c** display a LogP of 3.59 and 4.49 which were consistent with the lipophilicity criteria. This parameter, which is linked to both biological and physicochemical properties, is one of the most important properties required for drug development conditioning its absorption, distribution, potency and elimination.

In our previous work on **EA** analogues containing amide groups, we showed that the apoptosis was induced by activation of caspases [21]. We investigated herein if compounds **3a** and **3c** on HCT116 cell line followed the same mechanism of action by using one of the hallmark for apoptosis which is the loss of mitochondrial membrane potential (ΔΨm) through caspase-induced apoptosis (see experimental section) [35].

By the measurement of mitochondrial membrane potential (results presented in Figure 3) we observed that compounds **3a** and **3c** induced mitochondrial dysfunctions with significant effects beginning at a concentration of 5 and 10 µM for compound **3c** and at 10 µM for compound **3a**. This study provides some convincing evidence that compounds **3a** and **3c** caused caspase-induced apoptosis of HCT116 cells through mitochondrial dysfunction.

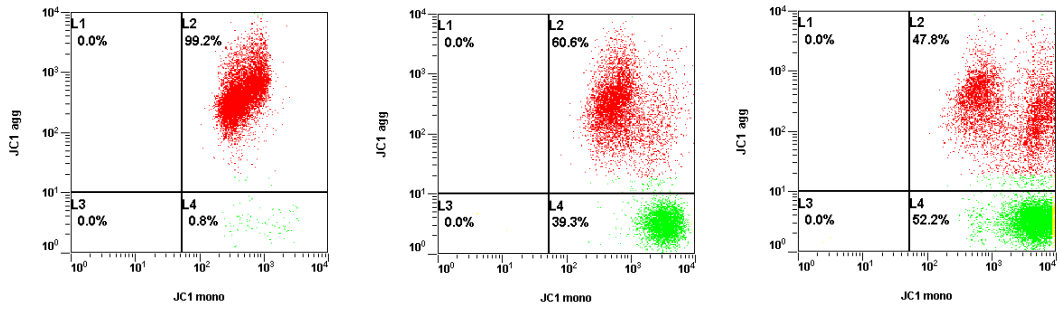

DMSO 5 µM of **3c** 10 µM of **3c**

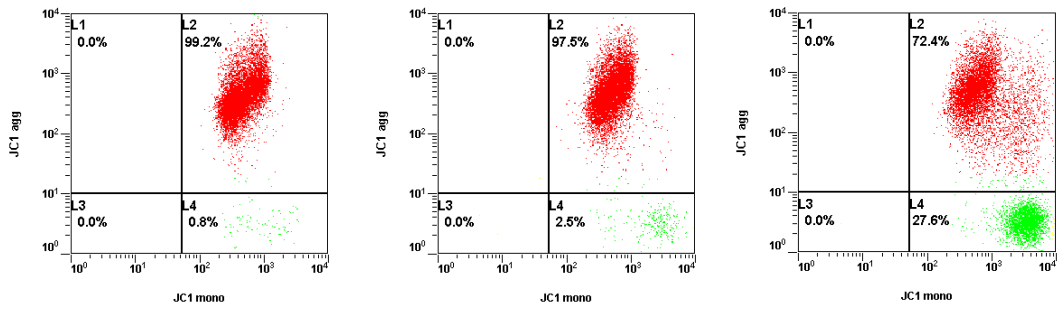

DMSO 5 µM of **3a** 10 µM of **3a**

Figure 3. Compounds **3a** and **3c** induced mitochondrial dysfunctions of HCT116 cells. Cells were incubated with **3a** or **3c** at either the concentrations of 5 or 10 µM for 24 h at 37°C. The portions of mitochondria dysfunction were measured using the JC-1 assay.

Glutathione is an abundant molecule regulating redox homeostasis in most mammalian cells[36]. As shown in Figure 4, we observed a reduction of the Mean Fluorescent Intensity in the cells treated with **3a** or **3c** at the concentration of 2 µM together with the appearance of a subpopulation of cells with a reduced GSH content compared with that of the control cells. These data indicated that both compounds induced a loss of reduced glutathione in treated cells which is an early hallmark in the progression of cell death.

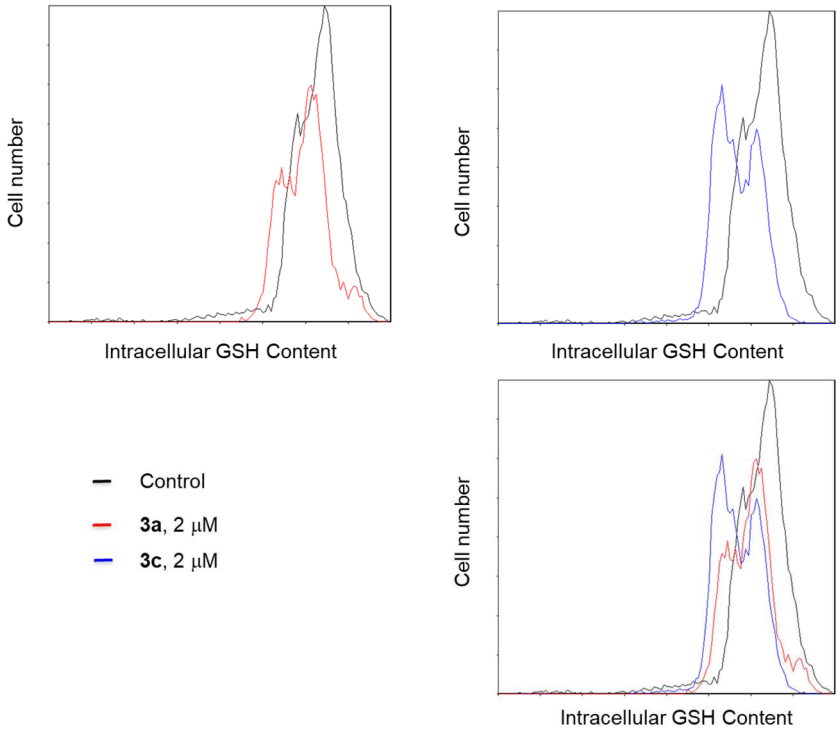

Figure 4. Compounds **3a** and **3c** induced the loss of reduced gluthatione in HCT116 cells. Cells were incubated with **3a** or **3c** at the concentration of 2 µM for 24 h at 37 °C. Intracellular GSH content was measured using GSH assay kit by flow cytometry.

3. Conclusion

In summary, copper (I)-catalyzed Azide-Alkyne Cycloaddition (CuAAC) reaction was used for an efficient synthesis of diverse **EA**-triazole derivatives. A series of **EA**-triazole compounds was designed and developed and new **EA** derivatives were screened for their *in vitro* activity against a panel of cancer cell lines as well as on a normal cell line. First a screening on HL60 cell line underlined that most of the compounds displayed excellent activity with IC_{50} less than 1 µM except for compound **3b** which displayed moderate activity with IC_{50} value of 1.73 µM. Subsequently, the most promising compounds **3a** and **3c** were selected for testing their *in vitro* anti-proliferative activities against others cancer cell lines (A549, MCF7, PC3, U87-MG, SKOV3 and HCT116) and against normal cell line (MRC5). The screening of their anti-proliferative activities led to the identification of compounds with evident selectivity for some cancer cell lines. Compound **3c** had a strong effective inhibitory activity *in vitro* against A549, PC3 and U87-MG with IC_{50} values of 20.2, 56.5 and 76.8 nM respectively, which were 2 fold more active than doxorubicin. Concerning compound **3a**, a good inhibitory activity was measured against A549 and PC3 with IC_{50} values of 50.1 and 92.5 nM respectively, which were similar or 2 fold more active than doxorubicin. Meanwhile, the selectivity index and lipophilicity were also investigated and compounds **3a** and **3a** were found to be more cytotoxic against A549 and PC3 cells than U87-MG cells with SI up to 82 fold and with good LogP. Our study showed also that compounds **3a** and **3c** caused a caspase-induced apoptosis of HCT116 cells through mitochondrial dysfunction. In addition, the measurement of intracellular GSH level revealed that compounds **3a** and **3c** induced a loss of reduced glutathione in HCT116 cells.

4. Experimental section

All chemicals, starting materials and solvents used in this study were bought from Fluorochem, Sigma-Aldrich or Alfa Aesar and used without further purification. Solvents mentioned as dry were purified with a dry station GT S100 immediately prior to use. The reactions were monitored by thin-layer chromatography (TLC) analysis by using silica gel (60 F254) plates. Compounds were visualized by ultraviolet (UV) irradiation at 254 or 365 nm. Column chromatography was performed on silica gel 60 (230–400 mesh, 0.040–0.063 mm). Melting points (m.p. [°C]) were taken on samples in open capillary tubes and are not corrected. The infrared spectra were recorded on a Thermo Scientific Nicolet iS10 are given in cm^{-1}. ^{1}H and ^{13}C NMR spectra were recorded on Bruker spectrometer at 400 MHz (^{13}C, 101 MHz). Chemical shifts are given in parts per million (ppm) from tetramethylsilane (TMS) as internal standard in $CDCl_3$, and the residual peak of DMSO in DMSO-d_6. The following abbreviations are used for the ^{1}H NMR spectra multiplicities: br. s: broad singlet, s: singlet, d: doublet, t: triplet, q: quartet, qt: quintuplet, m: multiplet. Coupling constants (*J*) are reported in Hertz [Hz]. High-resolution mass spectra (HRMS) were recorded with a Maxis Bruker 4G instrument and were performed in positive mode with an ESI source on a Q-TOF mass spectrometer with an accuracy tolerance of 2 ppm. The exact mass for chlorine containing molecules is given for the isotope 35.

4.1. Cell Culture and Proliferation Assay:

Cancer cell lines were obtained from the American Type Culture Collection (Rockville, MD, USA) or from the European collection of cell culture (ECACC, England) and were cultured according to the supplier's instructions. Human HCT-116 colorectal carcinoma, MCF7 breast adenocarcinoma, PC3 prostate adenocarcinoma, A549 lung carcinoma and SK-OV-3 ovary carcinoma were grown in Gibco McCoy's 5A supplemented with 10% fetal calf serum (FCS) and 1% glutamine. HL60 myelogenous leukemia cells were grown in RPMI 1640 supplemented with 10% fetal calf serum (FCS) and 1% glutamine. U87-MG glioblastoma and human MRC-5 cells were grown in Gibco medium DMEM supplemented with 10% fetal calf serum (FCS) and 1% glutamine. Cells were maintained at 37°C in a humidified atmosphere containing 5% CO_2. Cell growth inhibition was determined by an MTS assay according to the manufacturer's instructions (Promega, Madison, WI, USA). Briefly, the cells were seeded in 96-well plates (2.5×10^3cells/well) containing 100 μL of growth medium. After 24 h of culture, the cells were treated with the tested compounds at 10 different final concentrations. After 72 h of incubation, 20 μL of Cell Titer 96® AQ_{ueous} One Solution Reagent was added for 2 h before recording absorbance at 490nm with a spectrophotometric plate reader. The dose-response curves were plotted with Graph Prism software and the IC_{50} values were calculated

using the Graph Prism software from polynomial curves (four or five-parameter logistic equations).

4.2. Mitochondrial membrane potential assay

One of the hallmarks for apoptosis is the loss of mitochondrial membrane potential (ΔΨm). The changes in the mitochondrial potential were detected by 5,5',6,6'-tetrachloro-1,1',3,3'-tetraethylbenzimidazolylcarbocyanine iodide/chloride (JC-1), a cationic dye that exhibits potential dependent accumulation in mitochondria, indicated by fluorescence emission shift from red (590 nm) to green (525 nm). In brief, HCT116 cells were treated with different concentrations of compounds **3a** and **3c** for 24 h. After treatment, cells were re-suspended in 1 mL of PBS containing 2 µM final concentration JC-1 probe and incubated at 37°C for 15 min. Analysis of cells was performed on a FC500 flow cytometer (Beckman Coulter, France).

4.3. Intracellular glutathione (GSH) assay

HCT116 cells were initially seeded at a density 2 x 105 cells/well in 6-well plates and stabilized overnight. Next, cells were treated with different concentrations of 3a and 3c for 24 h. Cells were then harvested and washed with 1× PBS and intracellular GSH was quantified using an intracellular GSH assay kit (Abcam,Cambridge, UK) according to the manufacturer's instructions. The fluorescence intensity was measured (excitation, 490 nm; emission, 525 nm) using a FC500 flow cytometer (Beckman Coulter, France).

4.4. General procedure for preparation of triazole EA derivatives

4.4.1. 2-(2,3-Dichloro-4-(2-methylenebutanoyl)phenoxy)-N-(prop-2-yn-1-yl) acetamide (1)

To a mixture of EDC (0.56 g, 3.62 mmol, 1.1 equiv.), HOB*t* (0.55 g, 3.62 mmol 1.1 equiv.), DMAP (0.02 g, 0.165 mmol, 0.05 equiv.), and ethacrynic acid (1 g, 3.29 mmol, 1 equiv.) in dry DMF (5 mL), propargylamine (0.18 g, 3.29 mmol, 1 equiv.) was added at 0°C. The reaction mixture was stirred overnight at room temperature. Then, ethyl acetate (100 mL) was added and the organic layer was washed with H_2O (2 x 50 mL) and brine (3 x 50 mL), dried over anhydrous $MgSO_4$ and concentrated under reduced pressure. The crude residue was purified by flash chromatography, using DCM/EtOAc, (3:1) (v/v) as eluent to give the desired product **1** as a white solid (830 mg, 74%), **m.p.** 160-162°C. **^{1}H NMR** ($CDCl_3$, 400 MHz), δ 7.20 (d, $^3J_{HH}$ = 9.0 Hz, 1H, H_{ar}), 7.09 (br, 1H, NH), 6.88 (d, $^3J_{HH}$ = 9.0 Hz, 1H, H_{ar}), 5.96 (s, 1H, =CH), 5.59 (s, 1H, =CH), 4.61 (s, 2H, OCH_2), 4.18 (dd, $^3J_{HH}$ = 2.5, 5.3 Hz, 2H, NCH_2), 2.47 (q, $^3J_{HH}$ = 7.4 Hz, 2H, CH_2), 2.30 (t, $^3J_{HH}$ = 2.5 Hz, 1H, CH), 1.15 (t, $^3J_{HH}$= 7.4 Hz, 3H, CH_3). **^{13}C NMR** ($CDCl_3$, 101 MHz); δ 195.4, 166.5, 154.4, 150.1, 134.3, 131.4, 128.7,

127.2, 123.0, 111.0, 78.7, 72.5, 68.1, 28.9, 23.3, 12.3. **IR (neat)** *v* (cm^{-1}) 3340, 2150, 1650, 1642. **HRMS** (+ESI) *m/z*: $[M+H]^+$ calculated for $C_{16}H_{16}Cl_2NO_3$: 340.5017, found, 340.5016.

4.4.2. General procedure for the synthesis of intermediates 2a-i

The synthesis of the key intermediates compounds **2a-i** were prepared according to references [32,37–41].

4.4.3. General procedure for the synthesis of 3a-i

To a solution of **1** (0.1 g, 0.29 mmol, 1 equiv.) and corresponding aryl azides (0.32 mmol, 1.1 equiv.) in a mixture of *t*-BuOH/H_2O (2:1) (5 mL), $CuSO_4 \cdot 5H_2O$ (0.0007 g, 0.003 mmol, 0.01 equiv.) and sodium ascorbate (0.057 g, 0.29 mmol, 1 equiv.) were added. The reaction mixture was stirred at 60°C overnight. After completion of the reaction, the mixture was diluted with H_2O (50 mL) and extracted with EtOAc (2 x 25 mL), the combined organic phase was washed with brine, then dried over anhydrous Na_2SO_4, filtered and concentrated under vacuum. The crude product was purified by column chromatography by using DCM/ EtOAc as eluent.

4.4.4. N-((1-(4-Aminophenyl)-1H-1,2,3-triazol-4-yl)methyl)-2-(2,3-dichloro-4-(2-methylenebutanoyl)phenoxy)acetamide (3a)

DCM/EtOAc, 3:2 (v/v). White solid (84 mg, 60%), **m.p.** 170-171°C. **^{1}H NMR** ($CDCl_3$, 400 MHz), δ 7.89 (s, 1H, H_{ar}), 7.49 (d, $^3J_{HH}$ = 8.5 Hz, 2H, H_{ar}), 7.41 (br, 1H, NH), 7.19 (d, $^3J_{HH}$ = 9.0 Hz, 1H, H_{ar}), 6.87 (d, $^3J_{HH}$ = 9.0 Hz, 1H, H_{ar}), 6.77 (d, $^3J_{HH}$ = 8.5 Hz, 2H, H_{ar}), 5.96 (s, 1H, =CH), 5.59 (s, 1H, =CH), 4.74 (d, $^3J_{HH}$ = 6.0 Hz, 2H, NCH_2), 4.62 (s, 2H, OCH_2), 3.91 (br, 2H, NH_2), 2.48 (q, $^3J_{HH}$= 7.4 Hz, 2H, CH_2), 1.16 (t, $^3J_{HH}$= 7.4 Hz, 3H, CH_3). **^{13}C NMR** ($CDCl_3$, 101 MHz); δ 195.5, 166.9, 154.4, 150.1, 147.1, 144.2, 134.3, 131.5, 128.7, 128.5, 127.1, 123.1, 122.2 (2C), 120.6, 115.2 (2C), 110.9, 68.2, 34.7, 23.4, 12.3. **IR (neat)** *v* (cm^{-1}) 3394, 3392, 3390, 1659, 1603, 1483. **HRMS** (+ESI) *m/z*: $[M+H]^+$ calculated for $C_{22}H_{22}Cl_2N_5O_3$: 474.1094, found, 474.1093.

4.4.5. 2-(2,3-Dichloro-4-(2-methylenebutanoyl)phenoxy)-N-((1-(pyridin-2-yl)-1H-1,2,3-triazol-4-yl)methyl)acetamide (3b)

DCM/EtOAc, 3:2 (v/v). White solid (49 mg, 36%), **m.p.** 150-153°C. **^{1}H NMR** (Acetone-*d_6,* 400 MHz), δ 8.62 (s, 1H, H_{ar}), 8.59-8.57 (m, 1H, H_{ar}), 8.15-8.12 (m, 2H, H_{ar}), 8.98 (br, 1H, NH), 8.55-8.50 (m, 1H, H_{ar}), 7.34 (d, $^3J_{HH}$ = 9.0 Hz, 1H, H_{ar}), 7.23 (d, $^3J_{HH}$ = 9.0 Hz, 1H, H_{ar}), 6.02 (s, 1H, =CH), 5.60 (s, 1H, =CH), 4.83 (s, 2H, OCH_2), 4.69 (d, $^3J_{HH}$ = 6.0 Hz, 2H, CH_2), 2.49

(q, $^3J_{HH}$ = 7.4 Hz, 2H, CH_2), 1.13 (t, $^3J_{HH}$ = 7.4 Hz, 3H, CH_3). **^{13}C NMR** (Acetone-d_6, 101 MHz); δ 194.8, 166.8, 155.4, 150.1 (2C), 148.8, 145.8, 139.6, 133.6, 130.1, 128.1, 127.3, 123.8, 122.1, 119.4, 113.3, 111.8, 68.3, 34.4, 23.1, 11.9. **IR (neat)** *v* (cm^{-1}) 3389, 1662, 1600, 1590. **HRMS** (+ESI) *m/z*: $[M+H]^+$ calculated for $C_{21}H_{20}Cl_2N_5O_3$: 460.0937, found, 460.0936.

4.4.6. N-((1-Benzyl-1H-1,2,3-triazol-4-yl)methyl)-2-(2,3-dichloro-4-(2-methylenebutanoyl) phenoxy)acetamide (3c)

DCM/EtOAc, 3:2 (v/v). White solid (92 mg, 66%), **m.p.** 145-146°C. **^{1}H NMR** ($CDCl_3$, 400 MHz), δ 7.44 (s, 1H, H_{ar}), 7.35-7.29 (m, 4H, H_{ar}), 7.28-7.21 (m, 2H, H_{ar}), 7.10 (d, $^3J_{HH}$ = 9.0 Hz, 1H, H_{ar}), 6.78 (d, $^3J_{HH}$ = 9.0 Hz, 1H, H_{ar}), 5.91 (s, 1H, =CH), 5.53 (s, 1H, =CH), 5.46 (s, 2H, OCH_2), 4.58 (d, $^3J_{HH}$ = 6.0 Hz, 2H, NCH_2), 4.52 (s, 2H, NCH_2), 2.42 (q, $^3J_{HH}$= 7.4 Hz, 2H, CH_2), 1.10 (t, $^3J_{HH}$= 7.4 Hz, 3H, CH_3). **^{13}C NMR** ($CDCl_3$, 101 MHz); δ 195.5, 166.9, 154.4, 150.1, 144.4, 134.4, 134.2, 131.4, 129.1 (2C), 128.8, 128.7, 128.1 (2C), 127.0, 123.0, 122.1, 110.9, 68.2, 54.2, 34.7, 23.3, 12.3. **IR (neat)** *v* (cm^{-1}) 3394, 1666, 1605, 1482. **HRMS** (+ESI) *m/z*: $[M+H]^+$ calculated for $C_{23}H_{23}Cl_2N_4O_3$: 473,1141, found, 473,1136.

4.4.7. 2-(2,3-Dichloro-4-(2-methylenebutanoyl)phenoxy)-N-((1-(4-methoxybenzyl)-1H-1,2,3-triazol-4-yl)methyl)acetamide (3d)

DCM/EtOAc, 3:2 (v/v). White solid (117 mg, 79%), **m.p.** 151-152°C. **^{1}H NMR** ($CDCl_3$, 400 MHz), δ 7.45 (s, 1H, H_{ar}), 7.33 (br, 1H, NH), 7.24 (d, $^3J_{HH}$ = 8.5 Hz, 2H, H_{ar}), 7.16 (d, $^3J_{HH}$ = 9.0 Hz, 1H, H_{ar}), 6.91 (d, $^3J_{HH}$ = 8.5 Hz, 2H, H_{ar}), 6.84 (d, $^3J_{HH}$ = 9.0 Hz, 1H, H_{ar}), 5.96 (s, 1H, =CH), 5.59 (s, 1H, =CH), 5.45 (s, 2H, NCH_2), 4.63 (d, $^3J_{HH}$ = 6.0 Hz, 2H, NCH_2), 4.57 (s, 2H, OCH_2), 3.81 (s, 3H, OCH_3), 2.48 (q, $^3J_{HH}$= 7.4 Hz, 2H, CH_2), 1.16 (t, $^3J_{HH}$= 7.4 Hz, 3H, CH_3). **^{13}C NMR** ($CDCl_3$, 101 MHz) δ 195.5, 166.8, 159.9, 154.4, 150.1, 144.3, 134.2, 131.4, 129.7 (2C), 128.7, 127.0, 126.3, 123.1, 121.8, 114.5 (2C), 110.9, 68.2, 55.3, 53.8 , 34.7, 23.4, 12.3. **IR (neat)** *v* (cm^{-1}) 3392, 1662, 1600, 1486. **HRMS** (+ESI) *m/z*: $[M+H]^+$ calculated for $C_{24}H_{25}Cl_2N_4O_4$: 503.1247, found, 503.1247.

4.4.8. 2-(2,3-Dichloro-4-(2-methylenebutanoyl)phenoxy)-N-((1-(4-fluorobenzyl)-1H-1,2,3-triazol-4-yl)methyl)acetamide (3e)

DCM/EtOAc, 3:2 (v/v). White solid (105 mg, 73%), **m.p.** 147-149°C. **^{1}H NMR** ($CDCl_3$, 400 MHz), δ 7.49 (s, 1H, H_{ar}), 7.37 (br, 1H, NH), 7.32-7.28 (m, 2H, H_{ar}), 7.16 (d, $^3J_{HH}$ = 9.0 Hz, 1H, H_{ar}), 7.12-7.02 (m, 2H, H_{ar}), 6.84 (d, $^3J_{HH}$ = 9.0 Hz, 1H, H_{ar}), 5.96 (s, 1H, =CH), 5.58 (s, 1H, =CH), 5.49 (s, 2H, NCH_2), 4.63 (d, $^3J_{HH}$ = 6.0 Hz, 2H, NCH_2), 4.58 (s, 2H, OCH_2), 2.47 (q, $^3J_{HH}$= 7.4 Hz, 2H, CH_2), 1.15 (t, $^3J_{HH}$= 7.4 Hz, 3H, CH_3). **^{13}C NMR** ($CDCl_3$, 101 MHz); δ 195.5, 166.9, 164.1 (C, J_{CF}= 250.2 Hz), 154.4, 150.1, 144.5, 134.2, 131.4, 130.2, 130.5 (2CH, J_{CF}=

8.0 Hz), 128.7, 127.0, 123.0, 122.0, 116.8 (2CH, J_{CF}= 22.2 Hz), 110.9, 68.2, 53.4, 34.7, 23.3, 12.3. **IR (neat)** *v* (cm^{-1}) 3382, 1656, 1600, 1479. **HRMS** (+ESI) *m/z*: $[M+H]^+$ calculated for $C_{23}H_{22}Cl_2FN_4O_3$: 491,1047, found, 491,1042.

4.4.9. 2-(2,3-Dichloro-4-(2-methylenebutanoyl)phenoxy)-N-((1-(4-nitrobenzyl)-1H-1,2,3-triazol-4-yl)methyl)acetamide (3f)

DCM/EtOAc, 3:2 (v/v). White solid (103 mg, 67%). **m.p.** 152-155°C. **^{1}H NMR** ($CDCl_3$, 400 MHz), δ 8.23 (d, $^3J_{HH}$ = 8.5 Hz, 2H, H_{ar}), 7.59 (s, 1H, H_{ar}), 7.39 (br, 1H, NH), 7.43 (d, $^3J_{HH}$ = 8.5 Hz, 2H, H_{ar}), 7.17 (d, $^3J_{HH}$ = 9.0 Hz, 1H, H_{ar}), 6.85 (d, $^3J_{HH}$ = 9.0 Hz, 1H, H_{ar}), 5.97 (s, 1H, =CH), 5.64 (s, 2H, NCH_2), 5.58 (s, 1H, =CH), 4.66 (d, $^3J_{HH}$ = 6.0 Hz, 2H, NCH_2), 4.59 (s, 2H, OCH_2), 2.48 (q, $^3J_{HH}$= 7.4 Hz, 2H, CH_2), 1.16 (t, $^3J_{HH}$ = 7.4 Hz, 3H, CH_3). **^{13}C NMR** ($CDCl_3$, 101 MHz); δ 195.5, 167.0, 154.4, 150.1, 148.1, 145.0, 141.4, 134.4, 131.4, 128.8, 128.6 (2C), 127.1, 124.3 (2C), 123.0, 122.5, 110.9, 68.2, 53.1, 34.7, 23.3, 12.3. **IR (neat)** *v* (cm^{-1}) 3394, 1666, 1605, 1485, 1522, 1347. **HRMS** (+ESI) *m/z*: $[M+H]^+$ calculated for $C_{23}H_{22}Cl_2N_5O_5$: 518,0992, found, 518,0988.

4.4.10. 2-(2,3-Dichloro-4-(2-methylenebutanoyl)phenoxy)-N-((1-(pyridin-4-ylmethyl)-1H-1,2,3-triazol-4-yl)methyl)acetamide (3g)

DCM/EtOAc, 3:2 (v/v). White solid (101 mg, 72%), **m.p.** 161-163°C. **^{1}H NMR** ($CDCl_3$, 400 MHz) δ 8.64-8.62 (m, 2H, H_{ar}), 7.58 (s, 1H, H_{ar}), 7.40 (br, 1H, NH), 7.17 (d, $^3J_{HH}$ = 9.0 Hz, 1H, H_{ar}), 7.13 (d, $^3J_{HH}$ = 8.0 Hz, 2H, H_{ar}), 6.85 (d, $^3J_{HH}$ = 9.0 Hz, 1H, H_{ar}), 5.96 (s, 1H, =CH), 5.59 (s, 1H, =CH), 5.55 (s, 2H, NCH_2), 4.67 (d, $^3J_{HH}$ = 6.0 Hz, 2H, NCH_2), 4.59 (s, 2H, OCH_2), 2.49 (q, $^3J_{HH}$= 7.4 Hz, 2H, CH_2), 1.16 (t, $^3J_{HH}$= 7.4 Hz, 3H, CH_3). **^{13}C NMR** ($CDCl_3$, 101 MHz) δ 195.5 (C, C(=O)), 166.9, 154.4, 150.6 (2C), 150.2, 150.1, 144.9, 143.3, 134.3, 131.5, 128.7, 127.1, 122.6, 122.3, 122.1, 110.9, 68.2, 52.8, 34.7, 23.3, 12.3. **IR (neat)** *v* (cm^{-1}) 3390, 1666, 1605, 1595. **HRMS** (+ESI) *m/z*: $[M+H]^+$ calculated for $C_{22}H_{22}Cl_2N_5O_3$: 474.1094, found, 474.1093.

4.4.11. 2-(2,3-Dichloro-4-(2-methylenebutanoyl)phenoxy)-N-((1-(pyridin-2-ylmethyl)-1H-1,2,3-triazol-4-yl)methyl)acetamide (3h)

DCM/EtOAc, 3:2 (v/v). White solid (98 mg, 70%), **m.p.** 147-148°C. **^{1}H NMR** (CD_3CN, 400 MHz) δ 8.56 (d, $^3J_{HH}$ = 4.5 Hz, 1H, H_{ar}), 7.80-7.72 (m, 2H, H_{ar}), 7.38 (br, 1H, NH), 7.33-7.30 (m, 1H, H_{ar}), 7.25 (d, $^3J_{HH}$ = 8.5 Hz, 1H, H_{ar}), 7.22 (d, $^3J_{HH}$ = 9.0 Hz, 1H, H_{ar}), 7.03 (d, $^3J_{HH}$ = 9.0 Hz, 1H, H_{ar}), 6.03 (s, 1H, =CH), 5.63 (s, 2H, NCH_2), 5.61 (s, 1H, =CH), 4.66 (s, 2H, OCH_2), 4.54 (d, $^3J_{HH}$ = 6.0 Hz, 2H, NCH_2), 2.45 (q, $^3J_{HH}$ = 7.4 Hz, 2H, CH_2), 1.14 (t, $^3J_{HH}$ = 7.4 Hz, 3H, CH_3). **^{13}C NMR** (CD_3CN, 101 MHz) δ 195.5, 166.8, 155.1, 155.0, 150.1, 149.6,

137.2, 133.5, 130.2, 128.9, 127.3 (2C), 123.2, 123.0, 122.3, 122.2, 111.8, 68.3, 55.0, 34.3, 23.1, 11.92. **IR (neat)** *v* (cm^{-1}) 3388, 1666, 1600, 1587. **HRMS** (+ESI) *m/z*: $[M+H]^+$ calculated for $C_{22}H_{22}Cl_2N_5O_3$: 447.1094, found, 474.1093.

4.4.12. N-((1-(2-Cyclohexylethyl)-1H-1,2,3-triazol-4-yl)methyl)-2-(2,3-dichloro-4-(2-methylenebutanoyl)phenoxy)acetamide (3i)

DCM/EtOAc, 3:2 (v/v). White solid (114 mg, 78%), **m.p.** 123-125°C. **^{1}H NMR** ($CDCl_3$, 400 MHz) δ 7.56 (s, 1H, H_{ar}), 7.39 (br, 1H, NH), 7.18 (d, $^3J_{HH}$ = 9.0 Hz, 1H, H_{ar}), 6.86 (d, $^3J_{HH}$= 9.0 Hz, 1H, H_{ar}), 5.96 (s, 1H, =CH), 5.59 (s, 1H, =CH), 4.66 (d, $^3J_{HH}$ = 6.0 Hz, 2H, NCH_2), 4.60 (s, 2H, CH_2), 1.82-1.65 (m, 6H, $3CH_2$), 1.32-1.10 (m, 8H, CH, $2CH_2$ and CH_3), 1.10-0.92 (m, 2H, CH_2). **^{13}C NMR** ($CDCl_3$, 101 MHz) δ 195.5, 166.9, 154.4, 150.1, 143.9, 134.2, 131.4, 128.8, 127.1, 123.0, 121.9, 110.9, 68.2, 48.3, 37.6, 34.9, 34.7, 32.8 (2C), 26.3, 26.0 (2C), 23.3, 12.3. **IR (neat)** *v* (cm^{-1}) 3389, 1669, 1610, 1480. **HRMS** (+ESI) *m/z*: $[M+H]^+$ calculated for $C_{24}H_{31}Cl_2N_4O_3$: 493.1764, found, 493.1771.

4.4.13. 1-(2,3-Dichloro-4-hydroxyphenyl)butan-1-one (5)[34]

Anisole **4** (2 g, 11.36 mmol, 1 equiv.), and butanoyl chloride (1.45 g, 13.63 mmol, 1.5 equiv.) are dissolved in 50 mL of absolute DCM, and the mixture is cooled to 0 °C, then a solution of $AlCl_3$ (2.27 g, 17.04 mmol, 1.5 equiv.) in 25 mL of DCM was added within 30 min, and the mixture is stirred for 2 h. A total of 75 mL of DCM is removed by distillation and is substituted by the same amount of DCM. This procedure is repeated twice. An additional amount of 1.5 equiv. of $AlCl_3$ is added, and the mixture is heated under reflux for 5 h. The mixture is poured on ice and acidified with concentrated HCl to pH 1. Tartaric acid is added for the complexation of aluminum until the solution is cleared up. The solution is extracted with EtOAc, and the organic layer is washed with H_2O and KOH solution (10%). The EtOAc organic layer is dried with Na_2SO_4. The crude residue was purified by flash chromatography, using DCM as eluent, to furnish **5** as a white solid (2.05 g, 78%).**^{1}H NMR** ($CDCl_3$, 400 MHz) δ 7.41 (d, $^3J_{HH}$ = 9.0 Hz, 1H, H_{ar}), 7.02 (d, $^3J_{HH}$ = 9.0 Hz, 1H, H_{ar}), 6.02 (s, 1H, OH), 2.92 (t, $^3J_{HH}$= 2.4 Hz, 2H, CH_2), 1.76 (h, $^3J_{HH}$ = 7.4 Hz, 2H, CH_2), 1.00 (t, $^3J_{HH}$ = 7.4 Hz, 3H, CH_3).

4.4.14. 1-(2,3-Dichloro-4-(prop-2-yn-1-yloxy)phenyl)butan-1-one (6)

Phenol **5** (1.5 g, 6.46 mmol, 1 equiv.) is dissolved in THF. Then potassium *tert*-butoxide (1.45 g, 12.92 mmol, 2 equiv.), and a catalytic amount of KI (0.10 g, 0.64 mmol, 0.1 equiv.) are added. Then, an amount of propargyl bromide (2.30 g, 19.38 mmol, 3 equiv.) was added slowly. The mixture is stirred at 60 °C for 24 h, poured into H_2O, acidified to pH 1 with

concentrated HCl, and extracted with EtOAc. The organic layer is washed with 10% KOH, H_2O, and brine then dried with Na_2SO_4. The crude residue was purified by flash chromatography, using DCM/EtOAc, 4:1 (v/v) as eluent, to furnish **6** as an oil (1.48 g, 85%). **^{1}H NMR** ($CDCl_3$, 400 MHz), δ 7.38 (d, $^3J_{HH}$ = 9.0 Hz, 1H, H_{ar}), 7.05 (d, $^3J_{HH}$ = 9.0 Hz, 1H, H_{ar}), 4.83 (d, $^3J_{HH}$ = 2.5 Hz, 2H, OCH_2), 2.89 (t, $^3J_{HH}$ = 7.4 Hz, 2H, CH_2), 2.60 (t, $^3J_{HH}$ = 7.4 Hz, 1H, CH), 1.73 (h, $^3J_{HH}$ = 7.4 Hz, 2H, CH_2), 0.97 (t, $^3J_{HH}$ = 7.4 Hz, 3H, CH_3). **^{13}C NMR** ($CDCl_3$, 101 MHz); δ 202.0, 155.6, 134.3, 131.2, 127.1, 123.5, 111.3, 111.2, 77.0, 57.0, 44.7, 17.8, 13.7. **IR (neat)** *v* (cm^{-1}) 2100, 1668. **HRMS** (+ESI) *m/z*: $[M+H]^+$ calculated for $C_{13}H_{13}Cl_2O_2$: 271.0287, found, 271.0285.

4.4.15. 1-(2,3-Dichloro-4-(prop-2-yn-1-yloxy)phenyl)-2-methylenebutan-1-one (7)

To a solution of **6** (0.5 g, 1.85 mmol, 1 equiv.) and 37% formaldehyde solution (0.083 g, 2.77 mmol, 1.5 equiv.) in ethanol (35 mL), was added a solution of potassium carbonate (0.25 g, 1.85 mmol, 1 equiv.) in a mixed solution of H_2O (17 mL) and ethanol (10 mL). The mixture was refluxed for 24 h and decanted into hydrochloric acid solution (a mixture of concentrated HCl (5 mL) and H_2O (340 mL)) after cooling down to room temperature. The crude residue was purified by flash chromatography, using DCM/EtOAc, 4:1 (v/v) as eluent, to give **7** as a white solid (170 mg, 33%), **m.p.** 123-123°C. **^{1}H NMR** ($CDCl_3$, 400 MHz) δ 7.20 (d, $^3J_{HH}$ = 9.0 Hz, 1H, H_{ar}), 7.07 (d, $^3J_{HH}$ = 9.0 Hz, 1H, H_{ar}), 5.96 (s, 1H, =CH), 5.63 (s, 1H, =CH), 4.85 (d, $^3J_{HH}$ = 2.5 Hz, 2H, OCH_2), 2.60 (t, $^3J_{HH}$= 2.4 Hz, 1H, CH), 2.49 (q, $^3J_{HH}$= 7.4 Hz, 2H, CH_2), 1.17 (t, $^3J_{HH}$= 7.4 Hz, 3H, CH_3). **^{13}C NMR** ($CDCl_3$, 101 MHz) δ 195.9, 155.0, 150.2, 133.6, 131.3, 128.6, 126.7, 123.2, 111.2, 77.1, 76.9, 57.1, 23.4, 12.4. **IR (neat)** *v* (cm^{-1}) 2129, 1660. **HRMS** (+ESI) *m/z*: $[M+H]^+$ calculated for $C_{14}H_{13}Cl_2O_2$: 283.1507, found, 283.1509.

4.4.16. 1-(4-((1-Benzyl-1H-1,2,3-triazol-4-yl)methoxy)-2,3-dichlorophenyl)-2-methylenebutan-1-one (8)

Following general procedure for preparing **3a-i**, the crude residue was purified by flash chromatography, using DCM/EtOAc, 3:1 (v/v) as eluent, to furnish **8** as a white solid (91 mg, yield of 62%), **m.p.** 110-112°C. **^{1}H NMR** ($CDCl_3$, 400 MHz) δ 7.62 (s, 1H, H_{ar}), 7.43-7.36 (m, 3H, H_{ar}), 7.33-7.28 (m, 2H, H_{ar}), 7.16 (d, $^3J_{HH}$ = 9.0 Hz, 1H, H_{ar}), 7.11 (d, $^3J_{HH}$ = 9.0 Hz, 1H, H_{ar}), 5.94 (s, 1H, =CH), 5.62 (s, 1H, =CH), 5.56 (s, 2H, NCH_2), 5.33 (s, 2H, OCH_2), 2.48 (q, $^3J_{HH}$ = 7.4 Hz, 2H, CH_2), 1.15 (t, $^3J_{HH}$ = 7.4 Hz, 3H, CH_3). **^{13}C NMR** ($CDCl_3$, 101 MHz) δ 195.9, 155.6, 150.2 (2C), 134.2, 133.2, 131.1, 129.2 (2C), 128.9, 128.5, 128.1 (2C), 127.0, 123.0, 111.3 (2C), 63.5, 54.3, 23.4, 12.4. **IR** (neat) *v* (cm^{-1}) 1668, 1478. **HRMS** (+ESI) *m/z*: $[M+H]^+$ calculated for $C_{21}H_{20}Cl_2N_3O_2$: 416.0927, found, 416.0929.

Acknowledgments

This work was supported by Euromed University of Fes and Campus France and partially supported by Orléans University, CNRST, CNRS, Labex SynOrg (ANR-11-LABX-0029) and Labex IRON (ANR-11-LABX-0018-01), Region Centre Val de Loire and FEDER (TECHSAB, CHEMBIO).

Conflicts of Interest

The authors declare no conflict of interest

References:

[1] World Health Organization, Cancer, (n.d.). https://www.who.int/news-room/fact-sheets/detail/cancer (accessed May 12, 2021).

[2] M. Plummer, C. de Martel, J. Vignat, J. Ferlay, F. Bray, S. Franceschi, Global burden of cancers attributable to infections in 2012: A synthetic analysis, Lancet Glob. Health 4 (2016) e609–e616.

[3] C.Y. Huang, D.T. Ju, C.F. Chang, P. Muralidhar Reddy, B.K. Velmurugan, A review on the effects of current chemotherapy drugs and natural agents in treating non-small cell lung cancer, Biomedicine 7 (2017) 12–23.

[4] M.L. Frangione, J.H. Lockhart, D.T. Morton, L.M. Pava, G. Blanck, Anticipating designer drug-resistant cancer cells, Drug Discov. Today 20 (2015) 790–793.

[5] K. Johansson, M. Ito, C.M.S. Schophuizen, S. Mathew Thengumtharayil, V.D. Heuser, J. Zhang, M. Shimoji, M. Vahter, W.H. Ang, P.J. Dyson, A. Shibata, S. Shuto, Y. Ito, H. Abe, R. Morgenstern, Characterization of new potential anticancer drugs designed to overcome glutathione transferase mediated resistance, Mol. Pharmaceutics 8 (2011) 1698–1708.

[6] D.M. Townsend, K.D. Tew, The role of glutathione-S-transferase in anti-cancer drug resistance, Oncogene 22 (2003) 7369–7375.

[7] S. Singh, Cytoprotective and regulatory functions of glutathione S-transferases in cancer cell proliferation and cell death, Cancer Chemother. Pharmacol. 75 (2015) 1–15.

[8] L.M. Kauvar, A.S. Morgan, P.E. Sanderson, W.D. Henner, Glutathione based approaches to improving cancer treatment, Chem. Biol. Interact. 111–112 (1998) 225–238.

[9] M.L. O'Brien, K.D. Tew, Glutathione and related enzymes in multidrug resistance, Eur. J. Cancer 32 (1996) 967–978.

[10] A. De Luca, L.J. Parker, W.H. Ang, C. Rodolfo, V. Gabbarini, N.C. Hancock, F. Palone, A.P. Mazzetti, L. Menin, C.J. Morton, M.W. Parker, M. Lo Bello, P.J. Dyson, A structure-based mechanism of cisplatin resistance mediated by glutathione transferase P1-1, Proc. Natl. Acad. Sci. U. S. A. 116 (2019) 13943–13951.

[11] G. Zhao, C. Liu, R. Wang, D. Song, X. Wang, H. Lou, Y. Jing, The synthesis of α,β-unsaturated carbonyl derivatives with the ability to inhibit both glutathione S-transferase P1-1 activity and the proliferation of leukemia cells, Bioorg. Med. Chem. 15 (2007) 2701–2707.

[12] A.J. Oakley, J. Rossjohn, M. Lo Bello, A.M. Caccuri, G. Federici, M.W. Parker, The three-dimensional structure of the human Pi class glutathione transferase P1-1 in complex with the inhibitor ethacrynic acid and its glutathione conjugate, Biochemistry 36 (1997) 576–585.

[13] I. Zanellato, I. Bonarrigo, M. Sardi, M. Alessio, E. Gabano, M. Ravera, D. Osella, Evaluation of platinum-ethacrynic acid conjugates in the treatment of mesothelioma, ChemMedChem. 6 (2011) 2287–2293.

[14] K.G.Z. Lee, M. V. Babak, A. Weiss, P.J. Dyson, P. Nowak-Sliwinska, D. Montagner, W.H. Ang, Development of an efficient dual-Action GST-inhibiting anticancer platinum(IV) prodrug, ChemMedChem. 13 (2018) 1210–1217.

[15] K.D. Tew, A.M. Bomber, S.J. Hoffman, Ethacrynic acid and piriprost as enhancers of cytotoxicity in drug resistant and sensitive cell lines, Cancer Res. 48 (1988) 3622–3625.

[16] Y. Kim, S.M. Gast, T. Endo, D. Lu, D. Carson, I.G.H. Schmidt-Wolf, In vivo efficacy of the diuretic agent ethacrynic acid against multiple myeloma, Leuk. Res. 36 (2012) 598–600.

[17] S. Awasthi, S.K. Srivastava, H. Ahmad, G. A. Ansari Interactions of glutathione S-transferase with ethacrynic acid and its glutathione conjugate, Biochim. Biophys. Acta 1164 (1993) 173-178.

[18] L.A. Cazenave, J.A. Moscow, C.E. Myers, K.H. Cowan, Glutathione S-transferase and drug resistance, in: Ozols R.F. (eds) Drug Resistance in Cancer Therapy. Cancer Treatment and Research, Springer, Boston, MA, 1989, pp. 171–187.

[19] M. Schmidt, Y. Kim, S.-M. Gast, T. Endo, D. Lu, D. Carson, I.G.H. Schmidt-Wolf, Increased in vivo efficacy of lenalidomide and thalidomide by addition of ethacrynic acid, In Vivo 25 (2011) 325–33.

[20] P.J. O'Dwyer, F. LaCreta, S. Nash, P.W. Tinsley, R. Schilder, M.L. Clapper, K.D. Tew, L. Panting, S. Litwin, R.L. Comis, R.F. Ozols, Phase I study of thiotepa in combination with the glutathione transferase inhibitor ethacrynic acid, Cancer Res. 51 (1991) 6059–6065.

[21] S. Mignani, N. El Brahmi, S. El Kazzouli, L. Eloy, D. Courilleau, J. Caron, M.M. Bousmina, A.M. Caminade, T. Cresteil, J.P. Majoral, A novel class of ethacrynic acid derivatives as promising drug-like potent generation of anticancer agents with established mechanism of action, Eur. J. Med. Chem. 122 (2016) 656–673.

[22] Y.H. Su, L.W. Chiang, K.C. Jeng, H.L. Huang, J.T. Chen, W.J. Lin, C.W. Huang, C.S. Yu, Solution-phase parallel synthesis and screening of anti-tumor activities from fenbufen and ethacrynic acid libraries, Bioorg. Med. Chem. Lett. 21 (2011) 1320–1324.

[23] D. Lu, J.X. Liu, T. Endo, H. Zhou, S. Yao, K. Willert, I.G.H. Schmidt-Wolf, T.J. Kipps, D.A. Carson, Ethacrynic acid exhibits selective toxicity to chronic lymphocytic leukemia cells by inhibition of the Wnt/b-catenin pathway, PLoS ONE 4 (2009) e8294.

[24] L.-W. Chiang, K. Pei, S.-W. Chen, H.-L. Huang, K.-J. Lin, T.-C. Yen, C.-S. Yu, Combining a solution-phase derived library with in-situ cellular bioassay: Prompt screening of amide-forming minilibraries using MTT assay, Chem. Pharm. Bull. 57 (2009) 714–718.

[25] X. Yang, G. Liu, H. Li, Y. Zhang, D. Song, C. Li, R. Wang, B. Liu, W. Liang, Y. Jing, G. Zhao, Novel oxadiazole analogues derived from ethacrynic acid: Design, synthesis, and structure - activity relationships in inhibiting the activity of glutathione S-transferase P1-1 and cancer cell proliferation, J. Med. Chem. 53 (2010) 1015–1022.

[26] G. Liu, R. Wang, Y. Wang, P. Li, G. Zhao, L. Zhao, Y. Jing, Ethacrynic acid oxadiazole analogs induce apoptosis in malignant hematologic cells through downregulation of Mcl-1 and c-FLIP, which was attenuated by GSTP1-1, Mol. Cancer Ther. 12 (2013) 1837–1847.

[27] T. Li, G. Liu, H. Li, X. Yang, Y. Jing, G. Zhao, The synthesis of ethacrynic acid thiazole derivatives as glutathione S-transferase pi inhibitors, Bioorg. Med. Chem. 20 (2012) 2316–2322.

[28] G. Cynkowska, T. Cynkowski, A.A. Al-Ghananeem, H. Guo, P. Ashton, P.A. Crooks, Novel antiglaucoma prodrugs and codrugs of ethacrynic acid, Bioorg. Med. Chem. Lett. 15 (2005) 3524–3527.

[29] R. Wang, C. Li, D. Song, G. Zhao, L. Zhao, Y. Jing, Ethacrynic acid butyl-ester induces apoptosis in leukemia cells through a hydrogen peroxide-mediated pathway

independent of glutathione S-transferase P1-1 inhibition, Cancer Res. 67 (2007) 7856–7864.

[30] A. El Abbouchi, N. El Brahmi, M.A. Hiebel, J. Bignon, G. Guillaumet, F. Suzenet, S. El Kazzouli, Synthesis and biological evaluation of ethacrynic acid derivatives bearing sulfonamides as potent anti-cancer agents, Bioorg. Med. Chem. Lett. 30 (2020) 127426.

[31] I. Stengel, A. Mishra, N. Pootrakulchote, S.J. Moon, S.M. Zakeeruddin, M. Grätzel, P. Bäuerle, “click-chemistry” approach in the design of 1,2,3-triazolyl-pyridine ligands and their Ru(II)-complexes for dye-sensitized solar cells, J. Mater. Chem. 21 (2011) 3726–3734.

[32] S.K. Mamidyala, M.A. Cooper, Probing the reactivity of o-phthalaldehydic acid/methyl ester: Synthesis of N-isoindolinones and 3-arylaminophthalides, Chem. Commun. 49 (2013) 8407–8409.

[33] E. Bonandi, M.S. Christodoulou, G. Fumagalli, D. Perdicchia, G. Rastelli, D. Passarella, The 1,2,3-triazole ring as a bioisostere in medicinal chemistry, Drug Discov. Today 22 (2017) 1572–1581.

[34] U. Kaeppler, N. Stiefl, M. Schiller, R. Vicik, A. Breuning, W. Schmitz, D. Rupprecht, C. Schmuck, K. Baumann, J. Ziebuhr, T. Schirmeister, A new lead for nonpeptidic active-site-directed inhibitors of the severe acute respiratory syndrome coronavirus main protease discovered by a combination of screening and docking methods, J. Med. Chem. 48 (2005) 6832–6842.

[35] S. Pecnard, O. Provot, H. Levaique, J. Bignon, L. Askenatzis, F. Saller, D. Borgel, S. Michallet, M.C. Laisne, L. Lafanechère, M. Alami, A. Hamze, Cyclic bridged analogs of isoCA-4: Design, synthesis and biological evaluation, Eur. J. Med. Chem. 209 (2021) 112873.

[36] W. Li, T. Tian, W. Zhu, J. Cui, Y. Ju, G. Li, Metal-free click approach for facile production of main chain poly(bile acid)s, Polym. Chem. 4 (2013) 3057–3068.

[37] P. Cilliers, R. Seldon, F.J. Smit, J. Aucamp, A. Jordaan, D.F. Warner, D.D. N’Da, Design, synthesis and antimycobacterial activity of novel ciprofloxacin derivatives, Chem. Biol. Drug Des. 94 (2019) 1518-1536.

[38] J.J. Yang, W.W. Yu, L.L. Hu, W.J. Liu, X.H. Lin, W. Wang, Q. Zhang, P.L. Wang, S.W. Tang, X. Wang, M. Liu, W. Lu, H.K. Zhang, Discovery and characterization of 1 H-1,2,3-triazole derivatives as novel prostanoid EP4 receptor antagonists for cancer immunotherapy, J. Med. Chem. 63 (2020) 569–590.

[39] L. Bahsis, H. Ben El Ayouchia, H. Anane, A. Pascual-Álvarez, G. De Munno, M. Julve, S.-E. Stiriba, A reusable polymer-supported copper(I) catalyst for triazole

click reaction on water: An experimental and computational study, Appl. Organometal. Chem. 33 (2019) e4669.

[40] M. Wijtmans, C. De Graaf, G. De Kloe, E.P. Istyastono, J. Smit, H. Lim, R. Boonnak, S. Nijmeijer, R.A. Smits, A. Jongejan, O. Zuiderveld, I.J.P. De Esch, R. Leurs, Triazole ligands reveal distinct molecular features that induce histaine H4 receptor affinity and subtly govern H4/H3 subtype selectivity, J. Med. Chem. 54 (2011) 1693–1703.

[41] U. Kaeppler, N. Stiefl, M. Schiller, R. Vicik, A. Breuning, W. Schmitz, D. Rupprecht, C. Schmuck, K. Baumann, J. Ziebuhr, T. Schirmeister, A new lead for nonpeptidic active-site-directed inhibitors of the severe acute respiratory syndrome coronavirus main protease discovered by a combination of screening and docking methods, J. Med. Chem. 48 (2005) 6832–6842.

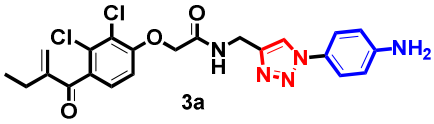

3a

IC_{50} = 50.1 nM on A549
SI = 33

IC_{50} = 50.1 nM on PC3
SI = 18

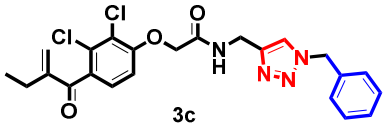

3c

IC_{50} = 20.2 nM on A549
SI = 82

IC_{50} = 56.5 nM on PC3
SI = 29

IC_{50} = 76.8 nM on U87
SI = 21